Heliyon 10 (2024) e30877

Contents lists available at ScienceDirect

Heliyon

journal homepage: www.cell.com/heliyon

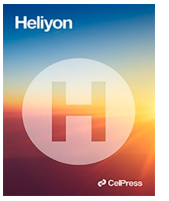

Research article

Construction of a novel disulfidptosis-related lncRNAs signature for prognosis prediction and anti-tumor immunity in laryngeal squamous cell carcinoma

Min Zhang [a,1], Qing Sun [b,1], Zhijin Han [c,1], Xuemei Qin [b], Tianle Gao [b], Yinwei Xu [b], Shuhui Han [b], Yujie Zhang [b], Qian Liang [d], Zhiqiang Guo [b], Jian Liu [b,*]

[a] *Xiangya Hospital, Central South University, Changsha, Hunan, 410000, PR China*
[b] *Department of Otolaryngology-Head and Neck Surgery, QingPu Branch of Zhongshan Hospital Affiliated to Fudan University, Shanghai, 201700, PR China*
[c] *Department of Otolaryngology, Peking Union Medical College Hospital, Chinese Academy of Medical Sciences and Peking Union Medical College, Beijing, 100730, PR China*
[d] *Department of Pathology, University of Texas Southwestern Medical Center, Dallas, TX, 75390, USA*

ARTICLE INFO

Keywords:
Disulfidptosis
Laryngeal squamous cell carcinoma
LncRNAs
Prognostic signatures
Anti-tumor immunity

ABSTRACT

Disulfidptosis, an innovative type of controlled cellular death linked to metabolic dysfunction, has garnered attention. However, there is limited knowledge regarding the involvement of disulfidptosisrelated lnRNAs (DRlncRNAs) in laryngeal squamous cell carcinoma (LSCC). The objective of our team in this study seeks to establish a DRlncRNAs signature, investigate their prognostic value in LSCC, and explore their associations with immune cell subpopulations, biological signaling pathways, and exploring implications for drug sensitivity. We accessed LSCC patients' RNA-seq data and pertinent clinical data for subsequent further analysis from The Cancer Genome Atlas (TCGA) portal. A literature search was conducted focusing on disulfidptosis-related genes. Pearson correlation coefficients were calculated to identify DRlncRNAs. Differential expression analysis of lncRNAs was performed. Utilizing univariate Cox regression analysis, we identified disulfidptosis-associated prognostic lncRNAs. The LASSO-Cox regression analysis was employed to refine this set of lncRNAs and construct a disulfidptosis-related lncRNAs signature. Various statistical techniques were employed to appraise model predictive performance. Subsequently, risk groups were stratified based on the risk score derived from the DRlncRNAs signature. The superiority of the risk score in prognostication over traditional clinicopathological features in LSCC patients was demonstrated. Evident distinctions emerged between risk groups, particularly in immune cell subpopulations like activated mast cells, eosinophils, and activated NK cells. Finally, the low-risk group demonstrated reduced IC50 values for specific chemotherapeutics like cisplatin and gemcitabine. The in vitro experiments indicated differential behavior of our DRlncRNAs. The DRlncRNAs signature can serve as a robust biomarker with the ability to predict both prognosis and therapeutic responses among patients with LSCC.

* Corresponding author.
E-mail address: Liujian_zZ@163.com (J. Liu).
[1] Min Zhang, Qing Sun and Zhijin Han are co-first authors and contribute equally to this work.

https://doi.org/10.1016/j.heliyon.2024.e30877
Received 1 March 2024; Received in revised form 9 April 2024; Accepted 7 May 2024
Available online 9 May 2024

1. Introduction

Laryngeal squamous cell carcinoma (LSCC), originating within the larynx, is a prominent variant of head and neck squamous cell carcinoma (HNSCC) observed globally [1]. LSCC is a predominant histologic subtype among laryngeal cancers, accounting for more than 90 % of cases [2]. Furthermore, it is ranked as the second most prevalent malignancy impacting both head-neck area and respiratory tract [3–5]. Although laryngeal cancer exhibits lower rates of incidence and mortality compared to other malignancies, there has been a concerning increase in these rates observed all over the world [6]. The most recent global cancer statistics report projected that more than 19,270 new cases of LSCC would been diagnosed, with 3980 deaths expected to happen in the United States alone [1]. Despite ongoing advancements in diagnosing and treating laryngeal cancer, there has been limited significant improvement in the overall survival rate due to the tumor characteristics with elusive incidence and high recurrence rate [7,8]. Hence, there is a pressing need to identify more efficient targets for both prediction and treatment.

The neologism "disulfidptosis" was introduced by Xiaoguang Liu and colleagues in their seminal article published in Nature Cell Biology earlier this year [9]. Disulfidptosis is a novel conception of programmed cell death associated with metabolic dysfunction. It arises from disulfide stress due to the buildup of disulfides that cannot be reduced within the intracellular environment [9]. This novel type of programmed cell death differs from cell death processes associated with oxidative stress such as apoptosis, ferroptosis, and necroptosis [10]. Liu et al. discovered that despite the knockdown of genes regulating apoptosis and ferroptosis, cell death still occurred but was inhibited by the thiol-based reducing agent Tris (2-Carboxyethyl) Phosphine (TCEP). Further investigation revealed that SLC7A11, highly expressed in cancer cells, facilitated cystine uptake, leading to glutathione synthesis to counteract oxidative stress from increased expression levels. However, during glucose deprivation, insufficient supply of nicotinamide adenine dinucleotide phosphate (NADPH) from the pentose phosphate pathway resulted in the inhibition of cysteine reduction to cysteine and an accumulation of intermolecular disulfide bonds in actin. This induced disulfide stress and activated the Rac-WAVE regulatory complex (WRC)-actin-related protein (Arp2/3) signaling pathway, culminating in cytoskeletal abnormalities and cell death [9]. Moreover, the metabolism of disulfides in cancer cells is associated with fundamental biological phenomena, including drug resistance, metastasis, and immune evasion [11–13]. As the origin of programmed cell death, it is anticipated that disulfidptosis could provide an innovative avenue for cancer metabolic therapy. This involves triggering disulfidptosis to target the vulnerabilities in cancer metabolism.

Long non-coding RNAs (lncRNAs) are RNA transcripts exceeding 200 nucleotides in length. They lack the functional role of encoding proteins but significantly contribute to the regulation of gene expression, chromatin remodeling, splicing, and intracellular transport [14]. Mounting evidence suggests that lncRNAs significantly influenced diverse cancer-related processes, including tumor initiation, proliferation, metastasis, drug resistance, and programmed cell death [15–17]. Currently, research investigating the modes of cell death in LSCC or HNSCC has identified immunity-related lncRNA [18], ferroptosis-related lncRNAs [19], MPT-driven necrosis-related [20], and stemness-related lncRNAs [21] as valuable prognostic biomarkers and therapeutic targets for LSCC or HNSCC. However, the role of DRlncRNAs remains unclear. Therefore, a comprehensive assessment of DRlncRNAs and the development

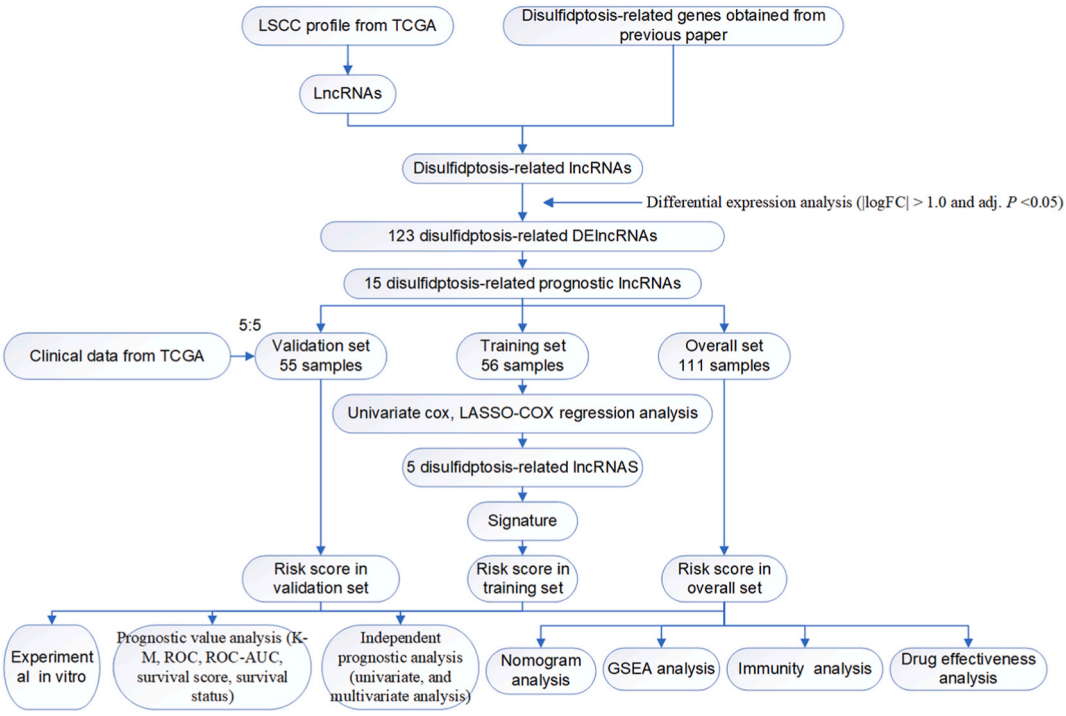

Fig. 1. The flow diagrams of the manuscript.

of prognostic markers are imperative for accurate clinical diagnosis and management. This includes monitoring prognostic markers, detecting disease progression early, and implementing appropriate therapeutic interventions to enhance patient survival and quality of life. Therefore, there is a pressing need to pinpoint prognostic DRlncRNAs specific to LSCC patients.

This study aimed to identify prognostic DRlncRNAs in LSCC, which can offer critical insights into the underlying signaling pathways and mechanisms involved in this process. Subsequently, this information can be used to formulate tailored approaches for drug treatments.

2. Materials and methods

Flow diagrams illustrating the methodology in this manuscript are presented in Fig. 1.

2.1. Collection and preparation of data

LSCC patients' RNA-sequencing (RNA-seq) data and available clinical related data were obtained from the TCGA database (https://portal.gdc.cancer.gov/) on March 23rd, 2023. We excluded samples that lacked survival information, then retrieved 12 adjacent non-cancerous tissue and 111 LSCC tumor tissue, along with the pertinent clinical information for these 111 LSCC patients. Additionally, we employed GENCODE lncRNA annotation (version 22) to delineate lncRNAs in the 111 LSCC patients [21,22]. Simultaneously, we searched the relevant candidate-gene literature to identify disulfidptosis-related genes (DRGs), from which we obtained 10 validated human DRGs [9].

2.2. Identification of disulfidptosis-related lncRNAs

To identify DRlncRNAs, we examined the correlation in expression patterns between these lncRNAs and genes linking to disulfidptosis, using Pearson correlation coefficients with a significance threshold of $P < 0.001$ and $|R| > 0.4$. Based on this analysis, we obtained that some lncRNAs were significantly correlated with DRGs.

2.3. Construction of the lncRNA-mRNA co-expression network

After DRlncRNAs were identified, we utilized Cytoscape software to construct a lncRNA−mRNA co-expression network by version 3.7.2. This analysis aimed to investigate the connections between potential target lncRNAs and their respective mRNAs. Additionally, we explored the characteristics of these predictive lncRNAs by creating Sankey diagrams via the "ggalluvial" R package.

2.4. Differential expression analysis

We conducted a search for potential prognostic lncRNAs that exhibited a connection to disulfidptosis and showed differential expression between adjacent non-cancerous tissue and LSCC tissue. The analysis was performed via the "limma" R package. To identify significant candidates, we applied a threshold of $|\log FC| > 1.0$ and adj. $P < 0.05$.

2.5. Development and validation of the prognostic signature for disulfidoptosis-related lncRNAs

We randomly divided 111 LSCC patients (the entire dataset) into training and validation sets according to a numerical ratio of 5:5. Using LSCC data extracted from the TCGA database, we employed univariate cox regression analysis to search for target lncRNAs ($P < 0.05$) within the training set. To mitigate the risk of overfitting associated with lncRNAs linked to disulfidptosis, we employed a appropriate statistical method, called the least absolute shrinkage and selection operator (LASSO)-Cox regression analysis. This approach allowed us to select the most relevant lncRNAs with significant associations. Subsequently, a prognostic model was developed utilizing multivariate cox regression analysis. Ultimately, we got an optimal prognostic model encompassed five robust lncRNAs. Furthermore, we calculated the risk score for each LSCC patient using the following computational formula: risk score $= \sum_{i=1}^{n}(\text{expi} * \beta\text{i})$. In this formula, "exp" represents the expression level of our target lncRNA, and "β" denotes its respective coefficient. LSCC patients within the training set were classified into either low-risk or high-risk groups, determined by the median score in its set. Moreover, the signature was assessed using several statistical methods. For assessing overall survival (OS) differences between the groups, Kaplan-Meier (KM) survival analysis was conducted by employing the "survminer" and "survival" R packages. The predictive performance of the developed model was gauged through calculation of the area under the receiver operating characteristic curve (ROC-AUC) via the "timeROC" R package. Moreover, the predictive capacity of the signature was further evaluated in both the validation and overall sets. Additionally, principal component analysis (PCA) was utilized to assess the distribution of expression patterns among the two groups. To examine the correlation between the risk score, including others clinical-pathological factors and OS in all LSCC patients, we employed univariate and multivariate cox regression analysis. We assessed the predictive accuracy of survival time by utilizing ROC curve through the "timeROC" R package. Finally, a nomogram was formulated to support clinical decision-making by integrating the DRlncRNAs signature along with other pertinent clinical factors, which served as a quantitative tool for evaluating clinical outcomes.

2.6. Conducting gene set enrichment analysis (GSEA)

To investigate biomolecular pathways differentiating the two groups utilizing the DRlncRNAs signature, we performed GSEA version 4.2.3 software [23]. This GSEA analysis was carried out via the "clusterProfiler" R package. Gene sets with $P < 0.01$ were deemed significantly enriched.

2.7. Analysis of immune infiltration

In order to evaluate immune infiltration in LSCC samples, we conducted a comparative analysis of 22 immune cell subtypes. These types encompass seven T cell subtypes, naive and memory B cells, plasma cells, and NK cells. We applied the CIBERSORT algorithm to compare their relative abundances across two distinct LSCC subgroups [24]. Subsequently, we proceeded to calculate the stromal, immune, and ESTIMATE scores for LSCC samples through the ESTIMATE algorithm via the "estimation" R package [25]. Furthermore, we employed the single sample gene set enrichment analysis (ssGSEA) with the "gsva" R package to identify 13 biomolecular signaling pathways related to immune distinguishing two separate LSCC subgroups [26]. Finally, we employed the Tumor Immune Dysfunction and Exclusion (TIDE) algorithm to find the underlying effectiveness of immune checkpoint blockade (ICB) therapy in LSCC patients ($P < 0.05$) [27].

2.8. Drug sensitivity analysis

Considering the survival benefits observed in LSCC patients with chemotherapy, our research endeavors were centered on the development of personalized chemotherapy regimens guided by risk scores. The aim was to optimize treatment efficacy for individuals diagnosed with LSCC. We calculated the half-maximal inhibitory concentration (IC50) via the "pRRophetic" R package to assess the response of each patient to chemotherapy [28].

2.9. Cell culturing

The human LSCC cell line (LCC) and the human immortalized keratinocyte cell line (HaCaT) were obtained from the Shanghai Cell Bank. Subsequently, the LCC and HaCaT cells were cultured in Roswell Park Memorial Institute medium (RPMI 1640), supplemented with 10 % fetal bovine serum (FBS) and 1 % penicillin-streptomycin. Cells were incubated at 37 °C with 5 % CO2 and 100 % humidity. Cell culture-related materials were purchased from Thermo Fisher Scientific.

2.10. Evaluation of the relative lncRNA expression in vitro experiment

Cellular RNA was isolated using Magen MagZol reagent (cat. No. R4801-01, Guangzhou, China), following the guidelines provided by the manufacturer. Complementary DNA (cDNA) was synthesized from messenger RNA (mRNA) using the Yeasen Hifair® III 1st Strand cDNA Synthesis SuperMix for qPCR (gDNA digester plus) Reverse Transcription System (cat. No. 11141ES10). Subsequently, quantitative PCR (qPCR) was conducted using 2× SYBR Green qPCR Master Mix (Low ROX) (Bimake, cat. No. B21702). PCR amplification reactions were performed using standard conditions: initial denaturation at 95 °C for 10 min, followed by 40 cycles of denaturation at 95 °C for 10 s, annealing at 60 °C for 30 s, extension at 95 °C for 15 s, 60 °C for 60 s, and final extension at 95 °C for 15 s. Specific primer sequences for the target lncRNAs and GAPDH were provided in Table 1. The relative quantification method ($2^{-\Delta\Delta Ct}$) was utilized to evaluate the relative lncRNA expression.

2.11. Statistical analysis

Statistical analyses were conducted using R software. The Wilcoxon test was utilized to compare two sets of paired data or ordinal

Table 1
The sequences of all primers.

Gene	Sequence	
GAPDH	Forward primer	CAACGGATTTGGTCGTATTGG
	Reverse primer	TGACGGTGCCATGGAATTT
AP003721.3	Forward primer	AGGAGGAAGAGGAGGAGGAGATG
	Reverse primer	AAGACCACACCATTGACCAAGAAG
AC040977.1	Forward primer	ACCCGCCGCTTTCTGTAGAG
	Reverse primer	CTGCCTGAGACCTATTTCGTGTTC
ODC1-DT	Forward primer	AGCAGGCACGACTTCCACAG
	Reverse primer	TCCGCATCACCACAGAATCAAAG
AL358334.2	Forward primer	TGTTGGCTGCTCCTGGCTTAC
	Reverse primer	GGTAATGCGAAGTTGCTGGTCTC
AC023310.4	Forward primer	TGCGATGTAGGAGCGGTAAGAC
	Reverse primer	GAAGGAGTGAGGAGGACAGGAAG

data. Pearson correlation analysis was employed to explore two sets of continuous numerical data in order to assess the strength and direction of the linear relationship between them. Kaplan-Meier analysis was used to evaluate survival analysis. Univariate cox regression analysis and multivariate cox regression analysis were used to examine significant prognostic factors and assess their independence. The ROC curve was used to evaluate the robustness of the risk score. Statistical significance was defined as $P < 0.05$.

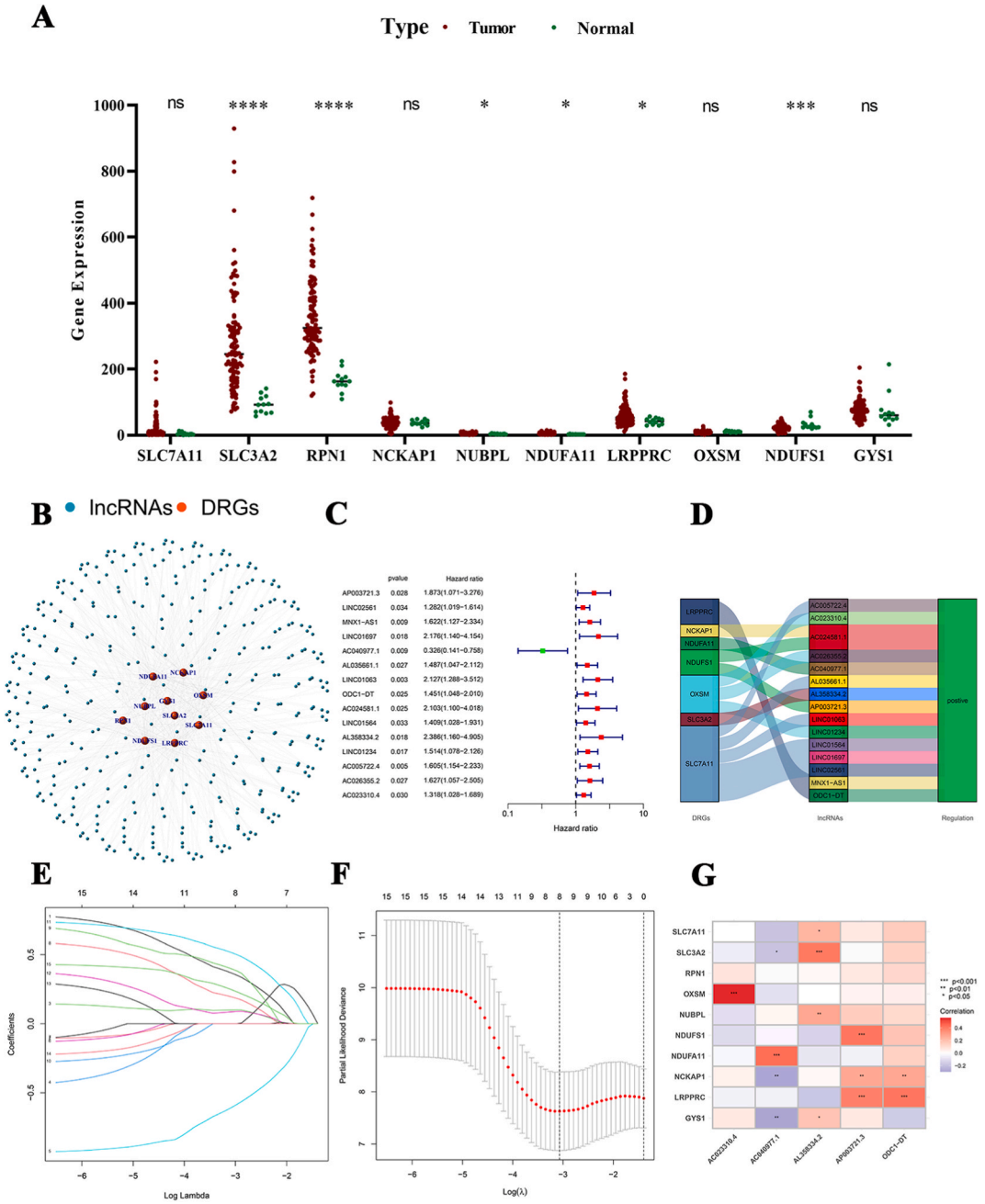

Fig. 2. Identification of disulfidptosis-related lncRNAs signature in LSCC. (A) The expression of 10 disulfdptosis-related genes between tumor tissues and normal tissues. (B) The network of DRGs and DRlncRNAs. (C) The forest plot of prognostic DRlncRNAs. (D) Sankey diagram of DRGs and DRlncRNAs. (E) LASSO coefficient profiles of DRlncRNAs. (F) The partial likelihood deviance with changing of log(λ). (G) Heatmap of DRGs and DRlncRNAs (*p < 0.05, **p < 0.01, ***p < 0.001, ****p < 0.0001, ns, no significance). Abbreviation: LSCC, laryngeal squamous cell carcinoma; DRGs, Disulfidptosis-related genes; DRlncRNAs, Disulfidptosis-related lncRNAs.

3. Results

3.1. Identification of disulfidptosis-related lncRNAs and construction of a prognostic disulfidptosis-related lncRNAs signature in LSCC

111 LSCC patients' RNA-seq data and corresponding clinical data were sourced from the TCGA database. 19938 mRNAs and 16876 lncRNAs were identified for the following analysis. We obtained DRGs (GYS1, NDUFS1, OXSM, LRPPRC, NDUFA11, NUBPL, NCKAP1, RPN1, SLC3A2, and SLC7A11) from the prior research [9]. Among these genes, SLC7A11, SLC3A2, RPN1, NUBPL, NDUFA11, LRPPRC, and GYS1 are highly expressed in laryngeal cancer tumor tissues, while the others show low expression in tumor tissues. The differences in expression levels of SLC3A2, RPN1, NUBPL, NDUFA11, LRPPRC, and NDUFS1 are statistically significant (Fig. 2A). The Pearson correlation analysis was conducted between lncRNAs and 10 genes related to disulfidptosis, we have identified a set of 377 lncRNAs, termed DRlncRNAs. We constructed a co-expression network of lncRNAs and genes, which elucidated the intricate associations between DRlncRNAs and DRGs (Fig. 2B). According to the criteria set, A total of 123 differentially expressed DRlncRNAs were identified as potential prognostic lncRNAs. Subsequently, the 111 cases of LSCC were randomly divided into two sets, called the training set (n = 56) and the validation set (n = 55) approximately maintaining a 5:5 ratio. Table 2 displayed the epidemiological and clinical characteristics of each patient with LSCC. Cox univariate regression analysis was applied to assess the prognostic capacity of these DRlncRNAs using the OS data of LSCC patients in the training set. As a result, 15 prognostic DRlncRNAs in LSCC were identified (Fig. 2C), and sankey diagram showed that all 15 lncRNAs individually enhance the expression levels of the specific DRGs they are connected to (Fig. 2D). Among these, only one DRlncRNA was classified as a "protective" gene, while the remaining DRlncRNAs were categorized as "risk" genes. In order to mitigate multicollinearity and ascertain 15 prognostic DRlncRNAs significantly correlated with OS of LSCC patients, LASSO Cox regression analysis was conducted. In the TCGA training set, five specific DRlncRNAs (AP003721.3, AC040977.1, ODC1-DT, AL358334.2, and AC023310.4) were utilized to build a risk score for predicting the OS of LSCC patients. The cvfit and lambda curves depicting the analysis results were presented in Fig. 2E and F, respectively. The risk score for each LSCC patient was calculated using the calculation formula: Risk score = AP003721.3 * 0.81563 + AC040977.1 * (−0.96433) + ODC1-DT * 0.35550 + AL358334.2 * 0.66679 + AC023310.4 * 0.44004. Additionally, the correlation heatmap emerged the relationships between these 5 DRlncRNAs and 10 DRGs (Fig. 2G).

Table 2
The clinical characteristics of LSCC patients in the training, validation and entire sets.

Characteristics	Entire	Validation	Training	*P*
Age				
≤65	73(65.77 %)	31(56.36 %)	42(75.00 %)	0.616
>65	38(34.23 %)	24(43.64 %)	14(25.00 %)	
Gender				
female	20(18.02 %)	10(18.18 %)	10(17.86 %)	> 0.999
male	91(81.98 %)	45(81.82 %)	46(82.14 %)	
Grade				
G1	8(7.21 %)	4(7.27 %)	4(7.14 %)	0.582
G2	70(63.06 %)	37(67.27 %)	33(58.93 %)	
G3	29(26.13 %)	12(21.82 %)	17(30.36 %)	
unknow	4(3.60 %)	2(3.64 %)	2(3.57 %)	
T classification				
T1	7(6.31 %)	4(7.27 %)	3(5.36 %)	0.924
T2	12(10.81 %)	5(9.09 %)	7(12.50 %)	
T3	25(22.52 %)	12(21.82 %)	13(23.21 %)	
T4	54(48.65 %)	27(49.09 %)	27(48.22 %)	
unknow	13(11.71 %)	7(12.73 %)	6(10.71 %)	
N classification				
N0	39(35.14 %)	21(38.18 %)	18(32.14 %)	0.521
N1	12(10.81 %)	6(10.91 %)	6(10.71 %)	
N2	39(35.14 %)	19(34.55 %)	20(35.71 %)	
N3	2(1.80 %)	0(0.00 %)	2(3.57 %)	
unknow	19(17.11 %)	9(16.36 %)	10(17.86 %)	
M classification				
M0	40(36.04 %)	26(47.27 %)	14(25.00 %)	0.778
M1	2(1.80 %)	0(0.00 %)	1(1.79 %)	
unknow	71(63.96 %)	29(52.73 %)	41(73.21 %)	
Stage				
I	2(1.80 %)	2(3.64 %)	0(0.00 %)	0.338
II	9(8.11 %)	3(5.45 %)	6(10.71 %)	
III	14(12.61 %)	8(14.55 %)	6(10.71 %)	
IV	71(63.96 %)	34(61.82 %)	37(66.08 %)	
unknow	15(13.51 %)	8(14.55 %)	7(12.50 %)	

3.2. Validation of the acquired model

The risk score for every LSCC patient in all datasets was computed using the above formula of the risk score and arranged in ascending order. Subsequently, all LSCC patients were categorized into two subgroups (high-risk and low-risk groups), based on whether their scores exceeded or were below the median scores observed in the training set, respectively. Fig. 3A–I illustrated the survival outcome, risk status, and lncRNA expression levels for each patient, individually presented for the training set, validation set, and the entire dataset. The results demonstrated a progressive rise in patient mortality with an escalating risk score. Kaplan-Meier analysis demonstrated significantly poorer OS in the high-risk group in contrast to the low-risk across all datasets (Fig. 3J, K and 3L). Our model exhibited greater predictive accuracy for LSCC survival, as evidenced by the ROC curve, which demonstrated AUC

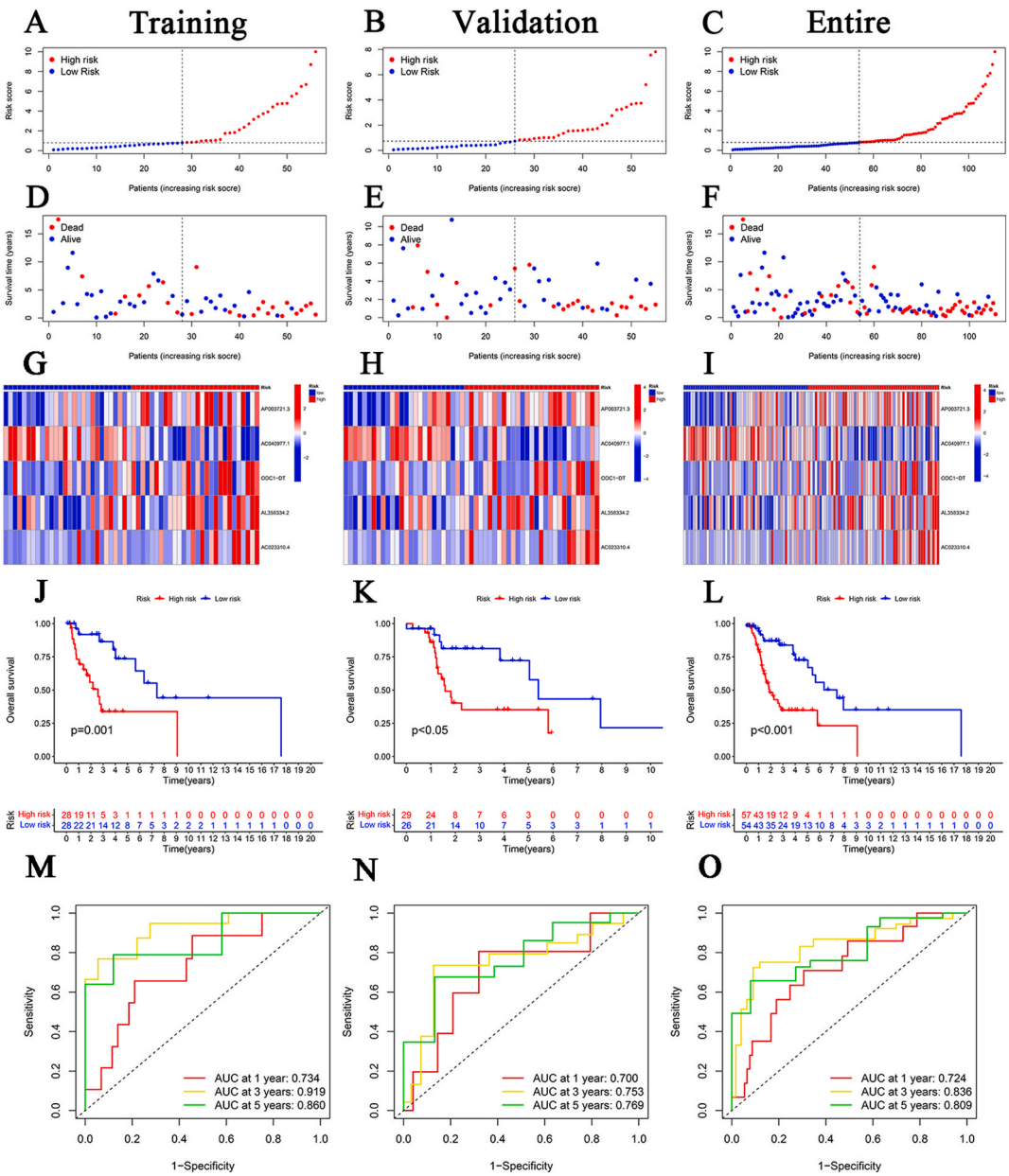

Fig. 3. Validation of the DRlncRNAs signature in the training, validation and entire sets. (A–I) The distribution of the risk scores, the distributions of the overall survival status and heatmap of the expression of 5 DRlncRNAs in the training, validation and entire sets. (J–L) Kaplan–Meier curves for the overall survival of patients in the high- and low-risk groups in the training, validation and entire sets. (M − O) The area under the time-dependent ROC curve (AUC) of the time-dependent receiver operating characteristic curve (ROC) verified the prognostic accuracy of the risk score in predicting 1-, 2-, and 3-year OS in the training, validation and entire sets. Abbreviation: DRlncRNAs, Disulfidptosis-related lncRNAs; OS, overall survival.

values of 0.736, 0.919, and 0.860 for one year, three years, and five years, respectively (Fig. 3M). In order to evaluate its predictive efficacy with greater precision, consistent findings were observed in two other sets, the testing set and the entire set ((Fig. 3N and O).

Next, to discuss the independent prognostic of the risk score, we conducted both univariate and multivariate cox regression analysis while incorporating clinical factors. Univariate cox regression analysis revealed gender (HR, 0.292; CI, 0.133–0.641; $P = 0.002$) and risk score (HR, 1.187; CI, 1.107–1.271; $P < 0.001$) exhibited a substantial correlation with OS (Fig. 4A). Furthermore, multivariate cox

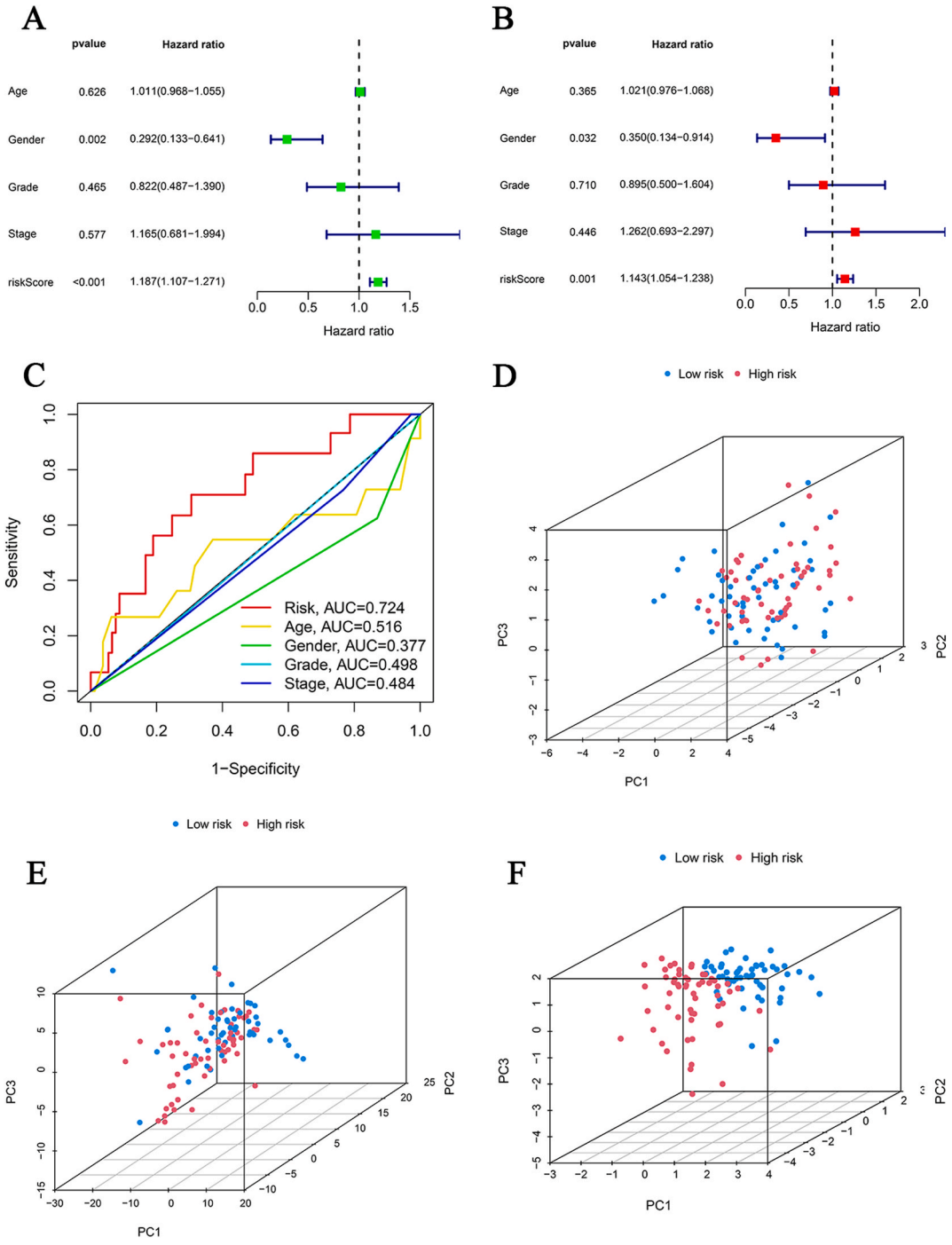

Fig. 4. The prognosis value of the novel DRlncRNAs signature. (A) The result of univariate cox regression analysis. (B) The result of multivariate cox regression analysis. (C) The ROC curves of risk score and clinical characteristics. (D) PCA of 10 DRGs expression. (E) PCA of 377 DRlncRNAs expression. (F) PCA of the prognostic 5 DRlncRNAs signature. Abbreviation: DRlncRNAs, Disulfidptosis-related lncRNAs; PCA, principal component analysis.

regression analysis indicated that gender (HR, 0.350; CI, 0.134–0.914; $P = 0.032$), and risk score (HR, 1.143; CI, 1.054–1.238; $P = 0.001$) could independent respectively predicted OS in LSCC patients (Fig. 4B). Subsequently, we evaluated the predictive specificity and sensitivity of risk scores in LSCC patients using the area under the curve (AUC), which showed higher values for risk scores compared to other clinicopathological factors (AUC = 0.724) (Fig. 4C). These findings emphasize the significance of five DRlncRNAs as crucial independent factors influencing the prognosis of LSCC. Furthermore, PCA was employed to find the differences between the two subgroups using 10 DRGs, 377 DRlncRNAs, and the risk models of the 5 DRlncRNAs, as illustrated in Fig. 4 D-F. The PCA results revealed that the analysis of the risk model (Fig. 4F) demonstrated a more distinct separation in opposite directions between the low-risk and high-risk groups compared to the other components (Fig. 4D and E). These findings suggest that the risk score effectively classifies LSCC patients into two distinct groups (low-risk and high-risk) with completely separate statuses.

3.3. Nomogram construction

The prognostic nomogram was developed by integrating a signature comprising 5 DRlncRNAs, as well as age, grade, gender, and stage, serving as predictive factors. Subsequently, the prognostic nomogram was employed to evaluate the prognostic outcomes of patients with LSCC at one, three and five years following diagnosis (Fig. 5A). And the calibration curves demonstrated satisfactory calibration (Fig. 5B).

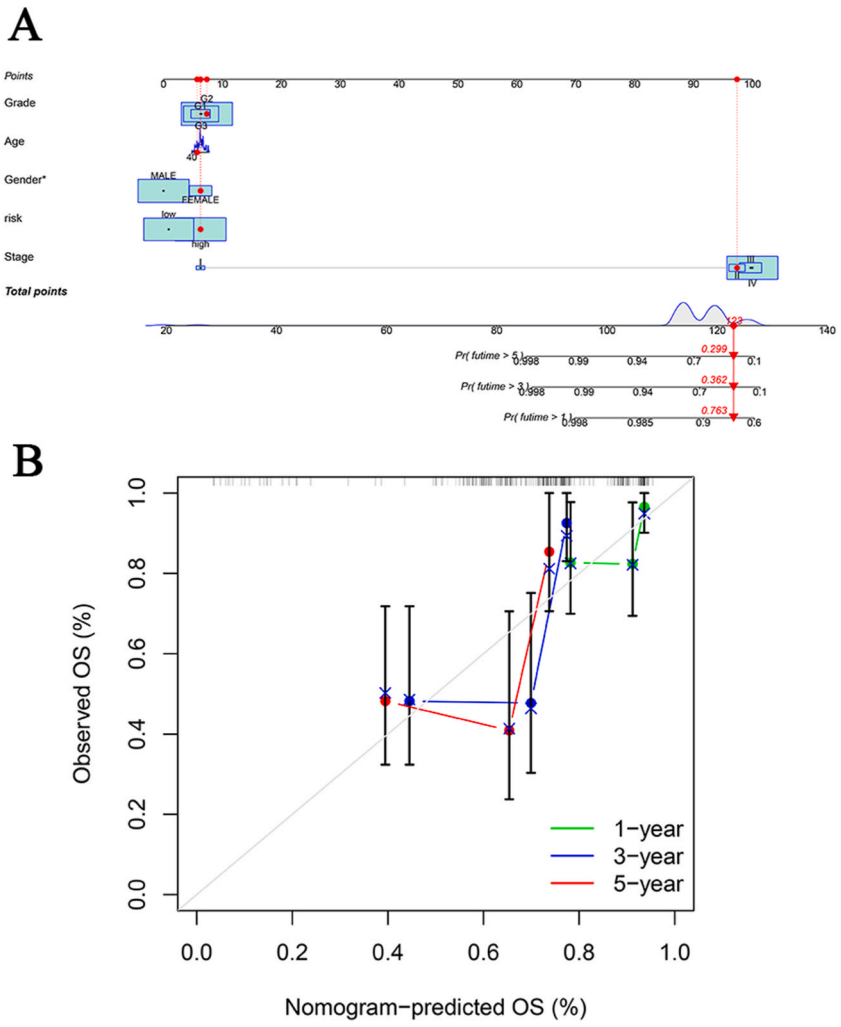

Fig. 5. Construction of nomogram models for LSCC
(A) A nomogram combining clinicopathological variables and risk score predicts the 1-, 3-, and 5- year overall survival. (B) The calibration curves for 1-, 3-, and 5-year OS.
(*p < 0.05, **p < 0.01, ***p < 0.001, ****p < 0.0001, ns, no significance). Abbreviation: LSCC, laryngeal squamous cell carcinoma; OS, overall survival.

3.4. The result of GSEA

GSEA was conducted to pinpoint pathways that were significantly enriched in both the two groups (high-risk and low-risk groups). Our GSEA results showed that a total of 144 out of 178 signaling pathways were upregulated, and 3 signaling pathways showed significant enrichment at a significance level of the nominal $P < 0.01$ in the high-risk group, on the other hand, in the low-risk group, a total of 34 out of 178 signaling pathways were upregulated, and 5 signaling pathways displayed significant enrichment at a significance level of the nominal $P < 0.01$. In the high-risk group, the enriched hallmark pathways included glutathione metabolism, pentose phosphate pathway, pentose and glucuronate interconversions. In contrast, the low-risk group predominantly exhibited enriched hallmark pathways related to immunity, such as intestinal immune network for IgA production, primary immunodeficiency, autoimmune thyroid disease, allograft rejection, and Type I diabetes mellitus in low-risk group (Fig. 6).

3.5. The result of tumor environment and immune infiltration

Immune cell infiltration in LSCC patients was evaluated by analyzing TCGA database data using the CIBERSORT algorithm. Significant discrepancies in the profiles of 22 infiltrating immune cell types were observed between the two groups (Fig. 7A). Furthermore, we observed considerably increased levels of activated mast cells and eosinophils in the high-risk group, while activated NK cell levels were significantly lower, upon comparing the immune cell proportions across different risk groups (Fig. 7B). Subsequently, we explored the correlation between infiltrating immune cells and 5 DRlncRNAs, as illustrated in Fig. 7C. Activated mast cells, eosinophils and activated NK cells conducted correlation analysis with risk score separately, we found that activated NK cells exhibited a decreasing trend with increasing risk scores, while activated mast cells and eosinophils displayed an increasing trend with higher risk score (Fig. 7D, E and 7F). Next, utilizing the ESTIMATE algorithm for immune infiltration assessment, the immune score of the high-risk group was notably lower than that of the low-risk group ($P < 0.01$) and it displayed a decreasing trend with escalating risk score ($R = -0.26$, $P = 0.0064$), as opposed to stromal scores and ESTIMATE scores ($R = -0.023$, $P = 0.81$; $R = -0.17$, $P = 0.072$) (Fig. 8).

The ssGSEA analysis of alterations in pathways related to immunofunction indicated that significantly elevated activity scores in various pathways, including APC co-inhibition, APC co-stimulation, CCR, check point, cytolytic activity, HLA, inflammation promoting, T cell co-inhibition and T cell co-stimulation, in the samples of the low-risk group (Fig. 9A). Subsequently, we assessed the expression changes of 43 common checkpoint genes across the two groups. Among them, PDCD1(PD-1), TNFRSF4, TNFRSF14, TNFRSF25, LAG3, CD40, CD244, CTLA4, TMIGD2, IDO2 and TIGIT exhibited increased expression, whereas HHLA2 displayed high expression in the high-risk group (Fig. 9B).

3.6. Evaluation of drug sensitivity common chemotherapeutics

The effectiveness of chemotherapy in enhancing the prognosis of LSCC patients is widely acknowledged, and common chemotherapy drugs include cisplatin, cetuximab, docetaxel, gemcitabine and paclitaxel [4]. Hence, by comparing the correlation between the risk score and the efficacy of these well-established anticancer drugs, we observed that individuals in the low-risk group demonstrated greater responsiveness to cisplatin and gemcitabine, compared to those in the high-risk group (Fig. 10). This finding may be helpful for personalized therapy for patients with LSCC.

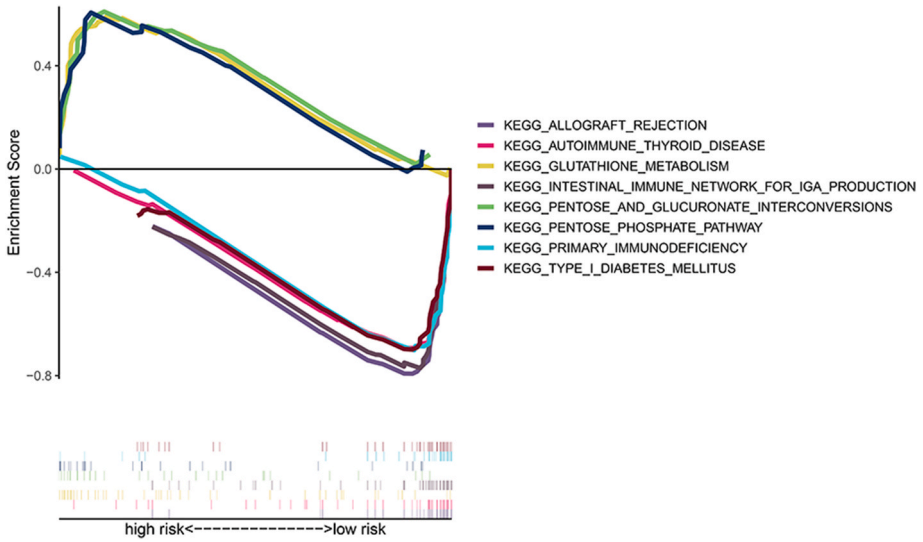

Fig. 6. Gene set enrichment analysis (GSEA) of t the high- and low-risk groups based on the risk score.

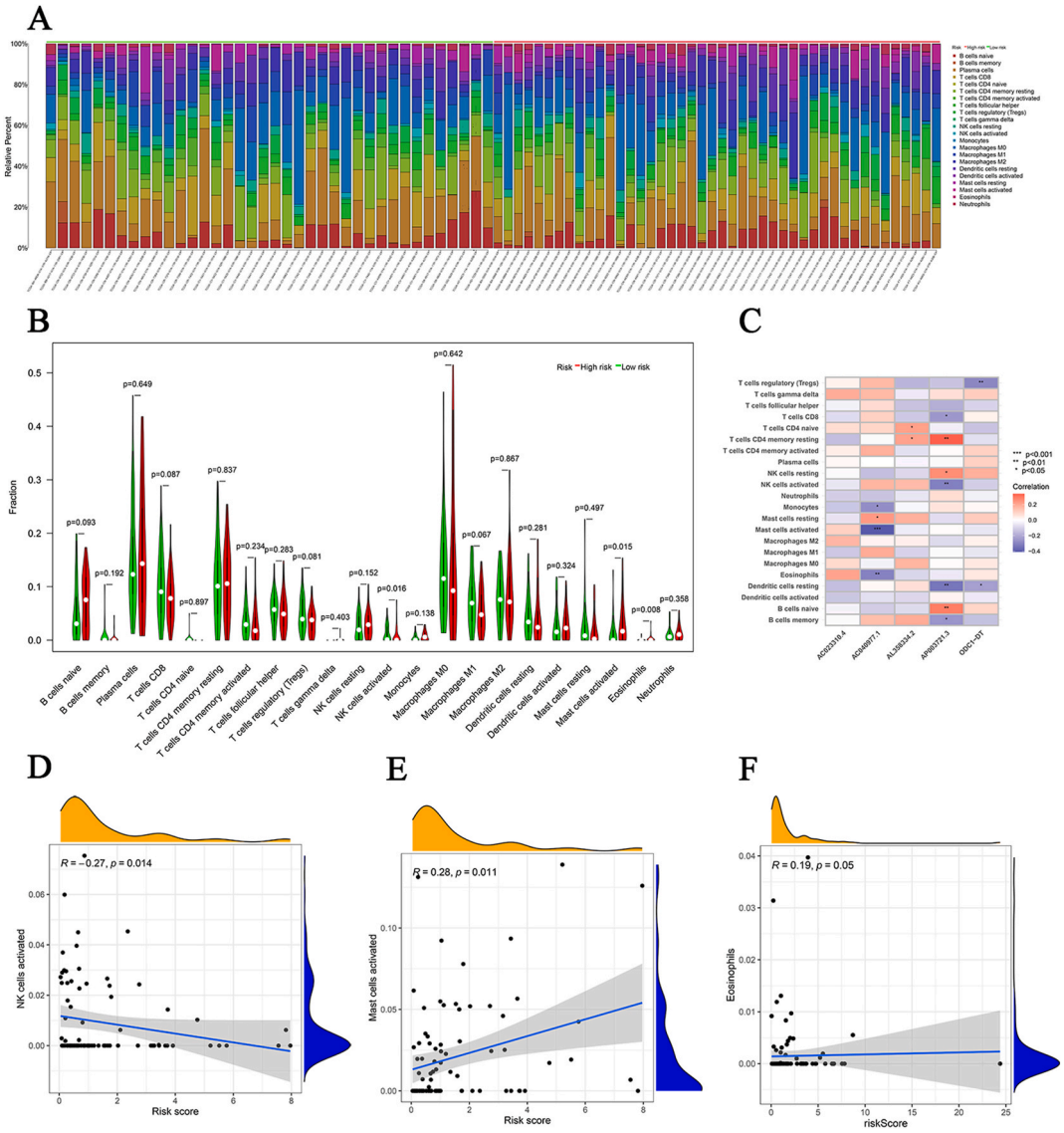

Fig. 7. Analysis of the immune cell infiltration in LSCC patients. (A) The proportions of 22 tumor infiltrating immune cells in individual LSCC patients by CIBERSORT analysis. (B) Violin diagram showing the immune cell composition between the two groups by CIBERSORT analysis. (C) Correlations between the 22 immune cell types and 5 DRlncRNAs in the model. (D–F) Correlation analysis between differentially expressed immune cells and the risk score (*$p < 0.05$, **$p < 0.01$, ***$p < 0.001$, ****$p < 0.0001$, ns, no significance). Abbreviation: LSCC, laryngeal squamous cell.

3.7. Investigation of the expression alterations about 5 DRlncRNA

Comprising five lncRNAs, our prognostic signature prompted an exploration of their expression levels in both TCGA LSCC cases and the LSCC cell line (LCC). The findings demonstrated that AC040977.1, ODC1-DT, AL358334.2 and AC023310.4 exhibited upregulation, while AP003721.3 displayed downregulation in the LSCC tumor tissue (Fig. 11A–E). Although the expression difference of AC040977.1 was not statistically significant, 5 DRlncRNAs demonstrated a similar trend of change in LCC (Fig. 11F–J). Thus, the above-mentioned findings demonstrated the robustness of our model and implied that these DRlncRNAs might have significant implications in LSCC.

4. Discussion

Laryngeal squamous cell carcinoma (LSCC) has exhibited new epidemiological characteristics in recent years. Among young individuals, particularly those under 40 years of age, the incidence rate of laryngeal cancer has observed a rise. This trend possibly due to factors such as shifting patterns in smoking and alcohol consumption, increased HPV infection rates, and unhealthy lifestyle choices

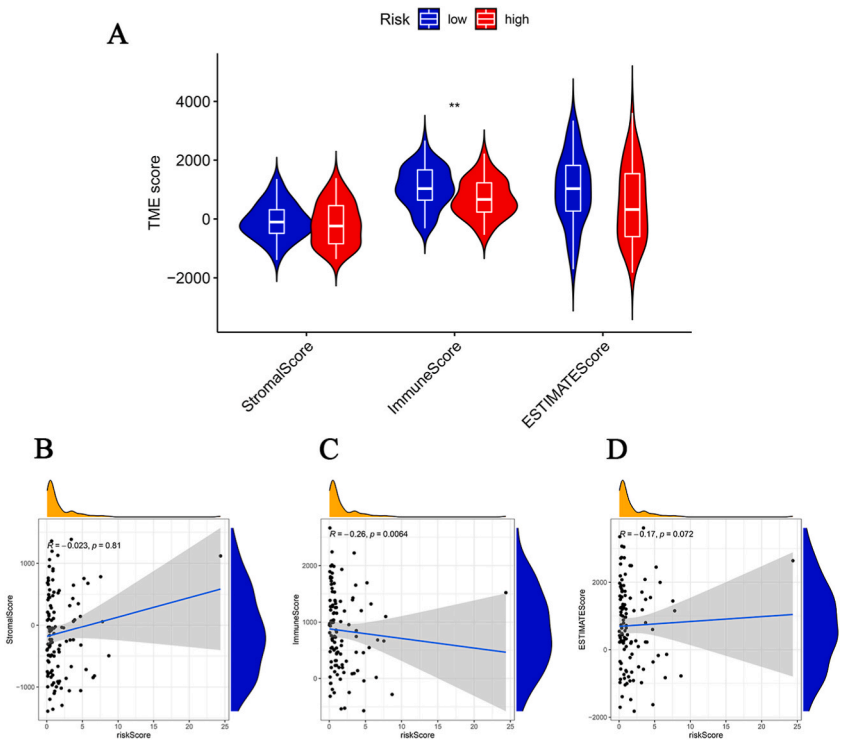

Fig. 8. Analysis of the immune cell infiltration in LSCC patients by ESTIMATE. (A) Stroma, immune, and ESTIMATE scores in the high-risk and low-risk groups in LSCC patients. (B–D) Correlation analysis between Stroma, immune, and ESTIMATE scores and the risk score. (*$p < 0.05$, **$p < 0.01$, ***$p < 0.001$, ****$p < 0.0001$, ns, no significance). Abbreviation: LSCC, laryngeal squamous cell.

[29]. Consequently, an urgent imperative exists to identify novel targets, devise early diagnostic methods, establish early prediction models, and offer appropriate therapeutic interventions. Discovered recently in 2023, disulfidptosis, a form of cell death, potentially unveils new strategies for the treatment of metabolic dysfunction in tumors [9]. Numerous researches have consistently demonstrated the crucial regulatory roles of lncRNAs during the initiation, progression, and metastasis processes of tumors [16], and previous studies have extensively documented the application of disulfidptosis-related lncRNAs (DRlncRNAs) signature in a variety of malignant tumors, including liver hepatocellular carcinoma [30], lung adenocarcinoma [31], and colon adenocarcinoma [32], revealing their significant prognostic and clinical utility. For example, chen et al. identified a six-DRlncRNAs signature of hepatocellular carcinoma, which could be a therapeutic biomarker for the treatment and prognosis of hepatocellular carcinoma patients [30]. Song et al. identified a five-DRlncRNAs signature for lung adenocarcinoma, which holds potential significance in predicting prognosis and optimizing treatment effects [31]. Nevertheless, no studies have investigated DRlncRNAs signature in LSCC.

This study utilized an analysis of 111 LSCC patient from the TCGA dataset to construct a 5-DRlncRNAs signature. Leveraging LASSO Cox regression analysis ensured dependable patient survival prediction in the training set. Based on derived risk score from the model, LSCC patients were categorized into high-risk and low-risk groups. KM survival analysis revealed notable survival disparities among patients with divergent risk scores. AUC-Curve of all LSCC patients verified the strong predictive ability of the 5-DRlncRNAs signature (the AUC value at 1, 3, and 5 years was 0.724, 0.836, and 0.809, respectively), which surpassed some of the existing models [33–35]. PCA further supported the disulfidptosis-related lncRNAs signature's ablities in differentiating high-risk from low-risk groups. univariate cox regression analysis and multivariate cox regression analysis both demonstrated that the risk score's autonomous influenced on OS. The forest plot of Hazard Ratio (HR) values (HR > 1) further confirmed that the risk score's role as an adverse factor. Furthermore, the model underwent validation in both the validation set and the entire dataset. Overall, the aforementioned analysis, in comparison to conventional clinical factors, substantiated the high reliability and effectiveness of the lncRNAs signature (AP003721.3, AC040977.1, ODC1-DT, AL358334.2, and AC023310.4) in predicting the SO of LSCC patients. Additionally, a nomogram was established, which serves as a tool for providing digital predictions to patients via calculations. The nomogram incorporated a five DRlncRNAs signature with clinical information. The results demonstrated a distinct concurrence between predicted OS and actual OS, indicating the nomogram's resilient predictive performance.

This finding suggested that some biological mechanisms among distinct risk score groups might diverge, which could explain the observed phenomena. To explore the potential mechanisms, we conducted further investigations into variations in functional enrichment about biological signaling pathways, immune-related signaling pathways functions and tumor microenvironment between the high-risk and low-risk groups. GSEA analysis result revealed that the high-risk group manifested activation of several signaling pathways associated with metabolic dysfunction in tumors, including glutathione metabolism, the pentose phosphate pathway, and

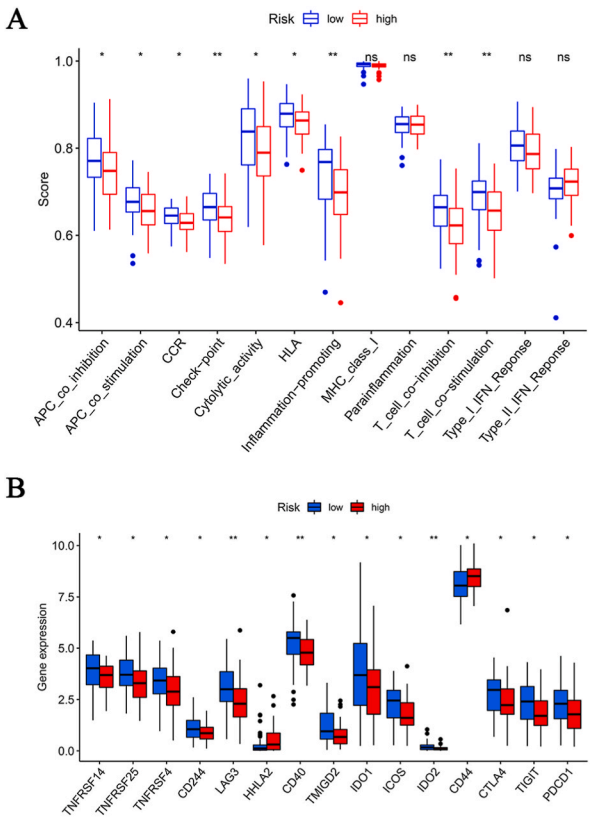

Fig. 9. Analysis of immune-related pathways in LSCC patients between the low-risk group and high-risk groups based on the ssGSEA scores. (A) Immune functional differences between the two groups. (B) The difference of common immune checkpoints expression in the two groups. (*$p <$ 0.05, **$p < 0.01$, ***$p < 0.001$, ****$p < 0.0001$, ns, no significance).

pentose and glucuronate interconversions. Conversely, the low-risk group showed activation of various signaling pathways associated with immune-related processes, such as the intestinal immune network for IgA production, autoimmune thyroid disease, primary immunodeficiency, allograft rejection and Type I diabetes mellitus. Immune cell infiltration results displayed notably increased levels of activated mast cells and eosinophils in the high-risk group compared to the low-risk group. In contrast, CIBERSORT analysis indicated significantly lower activated NK cell levels in the high-risk group. Additionally, our ESTIMATE analysis unveiled a considerably higher immune score in the low-risk group than in the high-risk group, indicating an enhanced immune cell infiltration in the former. Several studies have focused on the protumorigenic role of activated mast cells and eosinophils in HNSCC, correlating their abundant infiltration with unfavorable prognosis in cancer individuals [36–38]. These findings may account for the divergence in prognosis between the two groups.

Immunotherapy represents a groundbreaking advancement in cancer treatment, exhibiting promising outcomes for enhancing the prognosis of tumor patients across different stages, particularly those in advanced or recurrent stages of cancer [39,40]. Among the array of immunotherapy approaches, argeted immunotherapy has emerged as a particularly compelling therapeutic strategy in the field of cancer research [41]. Specifically, targeted therapy focusing on PD-1/PD-L1 inhibitors, such as pembrolizumab and nivolumab, has gained approval as a primary treatment option for advanced, or recurrent HNSCC patients, including LSCC patients [42–44]. The low-risk group exhibited heightened expression of diverse IBC, including PDCD1 (PD-1), CTLA4 and IDO1, in contrast to the high-risk group, which indicated that low-risk patients might attain obvious treatment responses when undergoing PD-1/PD-L1 inhibitors. Consequently, it is conceivable that LSCC patients with lower risk score are anticipated to experience improved survival outcomes after receiving immunotherapy, as suggested by our DRlncRNAs signature.

Next, our objective was to evaluate the correlation between the DRlncRNA signature and chemosensitivity in LSCC patients, achieved through the analysis of IC50 values. The above results demonstrated that individuals within the low-risk group displayed increased responsiveness to cisplatin and gemcitabine treatments compared to those within the high-risk group. This suggested that low-risk patients exhibited a higher susceptibility to disulfidptosis induced by chemotherapeutic drugs, underscoring the potential of the DRlncRNAs signature as a prognostic marker for chemosensitivity in LSCC. Finally, we evaluated the basal expression levels of these DRlncRNAs in the LSCC cell line and the TCGA LSCC lncRNAs. The result revealed these DRlncRNAs indicated their potential significance in LSCC.

Nonetheless, our study had inherent limitations. Firstly, our study exclusively utilized data from the TCGA database for both the training and validation sets. Incorporating external validation cohorts would not only bolster the validation process but also augment

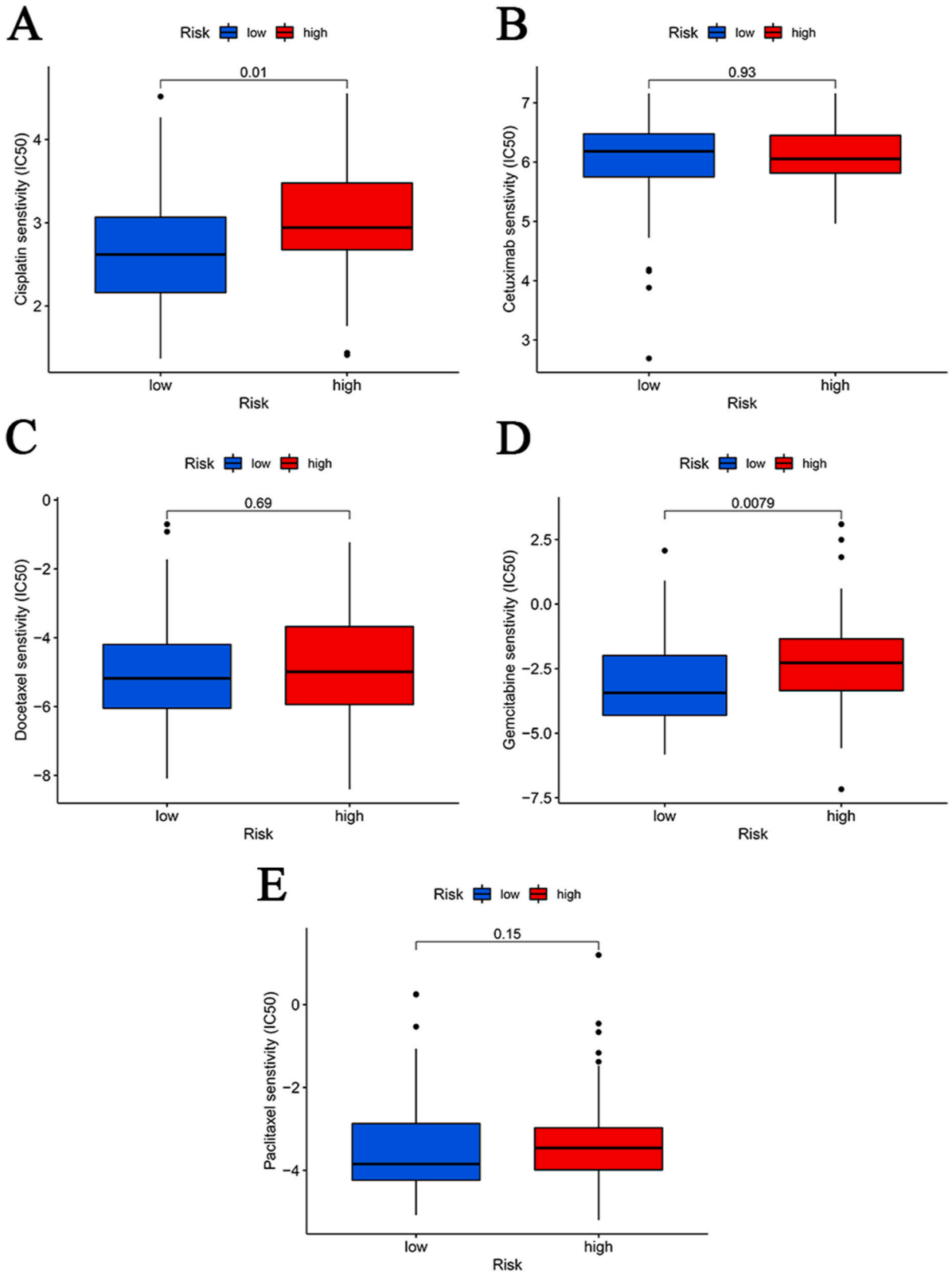

Fig. 10. The chemotherapeutic responses of the two groups to common anticancer drugs. (A) Cisplatin. (B) Cetuximab. (C) Docetaxel. (D) Gemcitabine. (E) Paclitaxel.

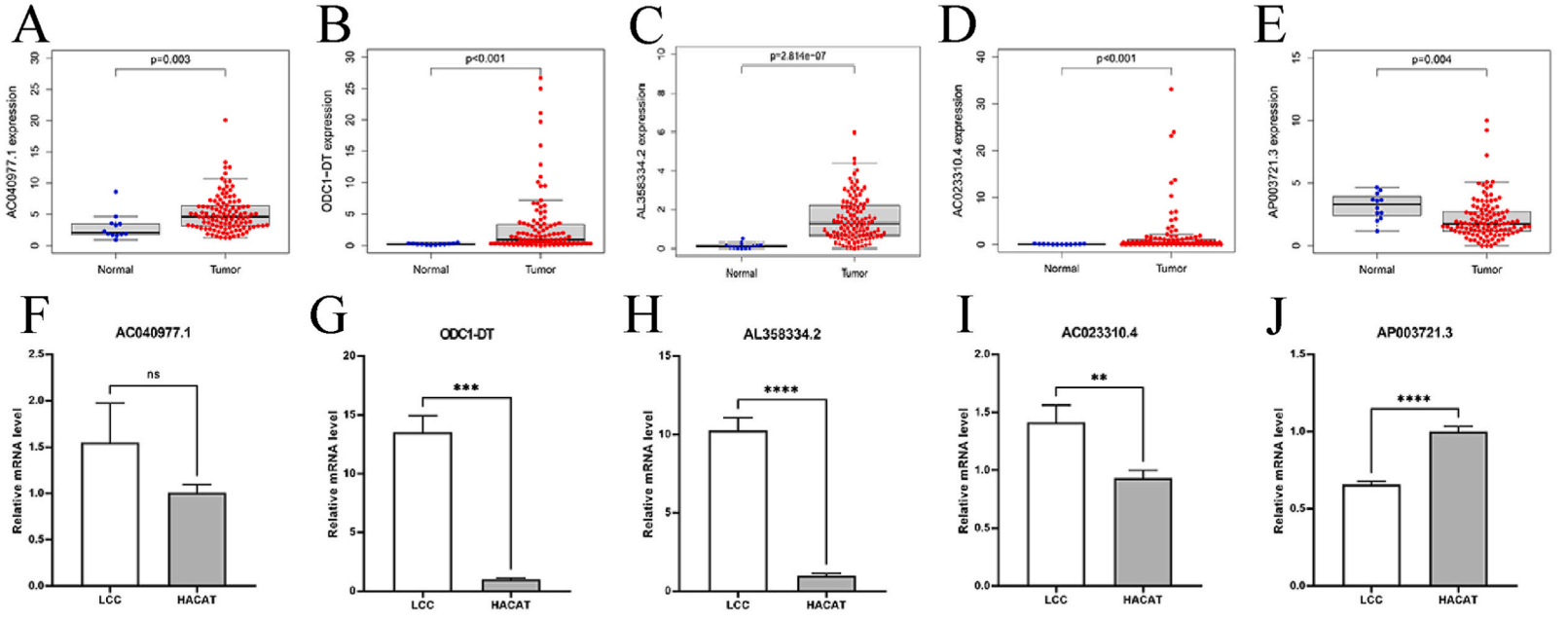

Fig. 11. The expression alterations of 5 DRlncRNAs. (A–E) The expression alterations of 5 DRlncRNAs in TCGA LSCC lncRNAs datebase. (E–J) The expression alterations of 5 DRlncRNAs in LSCC cell line (LCC). (*$p < 0.05$, **$p < 0.01$, ***$p < 0.001$, ****$p < 0.0001$, ns, no significance). Abbreviation: DRlncRNAs, Disulfidptosis-related lncRNAs.

the overall generalizability of our findings. Additionally, our study did not include a series of experiments intended to elucidate the underlying biological functions of DRlncRNAs. Therefore, future research should prioritize conducting rigorous experimental validation to gain further insights into these mechanisms.

5. Conclusion

We have developed a robust predictive model that utilizes five DRlncRNAs. This innovative model provides potential avenues to investigate the mechanisms involved in disulfidptosis. Additionally, it presents a novel treatment strategy for patients diagnosed with LSCC.

Funding

This work was funded by the Discipline Leader Training Program of Health Commission (WD2019-13, Qingpu District, Shanghai, PR China), the Project of Health Commission (W2021-03, Qingpu District, Shanghai, PR China) and the Hospital-level Project of QingPu Branch of Zhongshan Hospital Affiliated to Fudan University (QYT2021-02).

Data availability

The raw data used in this manuscript is accessible through the TCGA database (https://portal.gdc.cancer.gov/). For more comprehensive data, interested parties are welcome to contact the corresponding author.

Ethics approval

Ethical approval was no necessary because the raw data originated from the TCGA database.

Consent for publication

No.

CRediT authorship contribution statement

Min Zhang: Writing – original draft, Investigation. **Qing Sun:** Data curation. **Zhijin Han:** Formal analysis. **Xuemei Qin:** Investigation. **Tianle Gao:** Methodology. **Yinwei Xu:** Software. **Shuhui Han:** Software. **Yujie Zhang:** Validation, Software. **Qian Liang:** Visualization. **Zhiqiang Guo:** Writing – review & editing. **Jian Liu:** Writing – review & editing, Writing – original draft.

Declaration of competing interest

None of the authors have any conflicts of interest.

Acknowledgements

We extend our gratitude to the researchers and organizations at TCGA for their substantial contributions, providing invaluable data used in our analysis.

References

[1] R.L. Siegel, K.D. Miller, H.E. Fuchs, Jemal A cancer statistics, 2022, Ca - Cancer J. Clin. 72 (1) (2022) 7–33.
[2] C.E. Steuer, M. El-Deiry, J.R. Parks, K.A. Higgins, Saba NF an update on larynx cancer, Ca - Cancer J. Clin. 67 (1) (2017) 31–50.
[3] R. Nocini, G. Molteni, C. Mattiuzzi, G. Lippi, Updates on larynx cancer epidemiology, Chin. J. Cancer Res. 32 (1) (2020) 18–25.
[4] D.G. Pfister, S. Spencer, D. Adelstein, D. Adkins, Y. Anzai, D.M. Brizel, et al., Head and neck cancers, version 2.2020, NCCN clinical Practice guidelines in Oncology, J. Natl. Compr. Cancer Netw. 18 (7) (2020) 873–898.
[5] J. Liu, Q. Sun, J. Zhao, X. Qin, T. Gao, G. Bai, et al., Early death in supraglottic laryngeal squamous cell carcinoma: a population-based study, Ear Nose Throat J. 0 (0) (2022) 1–9.
[6] H. Sung, J. Ferlay, R.L. Siegel, M. Laversanne, I. Soerjomataram, A. Jemal, et al., Global cancer statistics 2020: GLOBOCAN Estimates of incidence and mortality Worldwide for 36 cancers in 185 countries, Ca - Cancer J. Clin. 71 (3) (2021) 209–249.
[7] S. Bock, S.J. Henley, M.E. O'Neil, S.D. Singh, T.D. Thompson, M. Wu, Cancer Distribution Among Asian, Native Hawaiian, and pacific islander subgroups - United States, 2015-2019, MMWR Morb. Mortal. Wkly. Rep. 72 (16) (2023) 421–425.
[8] R. Obid, M. Redlich, C. Tomeh, The treatment of laryngeal cancer, Oral Maxillofac. Surg. Clin. 31 (1) (2019) 1–11.
[9] X. Liu, L. Nie, Y. Zhang, Y. Yan, C. Wang, M. Colic, et al., Actin cytoskeleton vulnerability to disulfide stress mediates disulfidptosis, Nat. Cell Biol. 25 (3) (2023) 404–414.
[10] P. Zheng, C. Zhou, Y. Ding, S. Duan, Disulfidptosis: a new target for metabolic cancer therapy, J. Exp. Clin. Cancer Res. 42 (1) (2023) 103.
[11] Y. Wang, Y. Jiang, D. Wei, P. Singh, Y. Yu, T. Lee, et al., Nanoparticle-mediated convection-enhanced delivery of a DNA intercalator to gliomas circumvents temozolomide resistance, Nat. Biomed. Eng. 5 (9) (2021) 1048–1058.
[12] S. Shrihari, H.C. May, J.J. Yu, S.B. Papp, J.P. Chambers, M.N. Guentzel, et al., Thioredoxin-mediated alteration of protein content and cytotoxicity of Acinetobacter baumannii outer membrane vesicles, Exp Biol Med (Maywood) 247 (3) (2022) 282–288.

[13] J. Zhang, X. Li, Z. Zhao, W. Cai, J. Fang, Thioredoxin signaling pathways in cancer, Antioxid Redox Signal 38 (4–6) (2023) 403–424.
[14] K.C. Wang, H.Y. Chang, Molecular mechanisms of long noncoding RNAs, Mol Cell 43 (6) (2011) 904–914.
[15] W. Xue, Y. Zheng, Z. Shen, L. Li, Z. Fan, W. Wang, et al., Involvement of long non-coding RNAs in the progression of esophageal cancer, Cancer Commun. 41 (5) (2021) 371–388.
[16] M. Ahmad, L.B. Weiswald, L. Poulain, C. Denoyelle, M. Meryet-Figuiere, Involvement of lncRNAs in cancer cells migration, invasion and metastasis: cytoskeleton and ECM crosstalk, J. Exp. Clin. Cancer Res. 42 (1) (2023) 173.
[17] H. Kitajima, R. Maruyama, T. Niinuma, E. Yamamoto, A. Takasawa, K. Takasawa, et al., TM4SF1-AS1 inhibits apoptosis by promoting stress granule formation in cancer cells, Cell Death Dis. 14 (7) (2023) 424.
[18] L. Qian, T. Ni, B. Fei, H. Sun, H. Ni, An immune-related lncRNA pairs signature to identify the prognosis and predict the immune landscape of laryngeal squamous cell carcinoma, BMC Cancer 22 (1) (2022) 545.
[19] Y. Tang, C. Li, Y.J. Zhang, Z.H. Wu, Ferroptosis-Related Long Non-Coding RNA signature predicts the prognosis of Head and neck squamous cell carcinoma, Int. J. Biol. Sci. 17 (3) (2021) 702–711.
[20] J. Liu, M. Zhang, Q. Sun, X. Qin, T. Gao, Y. Xu, et al., Construction of a novel MPT-driven necrosis-related lncRNAs signature for prognosis prediction in laryngeal squamous cell carcinoma, Environ. Sci. Pollut. Res. Int. 30 (31) (2023) 77210–77225.
[21] Xu Z., Zhang M., Guo Z., Chen L., Yang X., Li X., et al., Stemness-related lncRNAs signature as a biologic prognostic model for head and neck squamous cell carcinoma, Apoptosis 28 (5-6) (2023) 860-880.
[22] A. Frankish, M. Diekhans, A.M. Ferreira, R. Johnson, I. Jungreis, J. Loveland, et al., GENCODE reference annotation for the human and mouse genomes, Nucleic Acids Res. 47 (D1) (2019) D766–d773.
[23] A. Subramanian, P. Tamayo, V.K. Mootha, S. Mukherjee, B.L. Ebert, M.A. Gillette, et al., Gene set enrichment analysis: a knowledge-based approach for interpreting genome-wide expression profiles, Proc. Natl. Acad. Sci. U.S.A. 102 (43) (2005) 15545–15550.
[24] B. Chen, M.S. Khodadoust, C.L. Liu, A.M. Newman, A.A. Alizadeh, Profiling tumor infiltrating immune cells with CIBERSORT, Methods Mol. Biol. 1711 (2018) 243–259.
[25] K. Yoshihara, M. Shahmoradgoli, E. Martínez, R. Vegesna, H. Kim, W. Torres-Garcia, et al., Inferring tumour purity and stromal and immune cell admixture from expression data, Nat. Commun. 4 (2013) 2612.
[26] M.S. Rooney, S.A. Shukla, C.J. Wu, G. Getz, N. Hacohen, Molecular and genetic properties of tumors associated with local immune cytolytic activity, Cell 160 (1–2) (2015) 48–61.
[27] P. Jiang, S. Gu, D. Pan, J. Fu, A. Sahu, X. Hu, et al., Signatures of T cell dysfunction and exclusion predict cancer immunotherapy response, Nat. Med. 24 (10) (2018) 1550–1558.
[28] P. Geeleher, N. Cox, Huang RS pRRophetic: an R package for prediction of clinical chemotherapeutic response from tumor gene expression levels, PLoS One 9 (9) (2014) e107468.
[29] S. Marur, G. D'Souza, W.H. Westra, A.A. Forastiere, HPV-associated head and neck cancer: a virus-related cancer epidemic, Lancet Oncol. 11 (8) (2010) 781–789.
[30] C. Chen, C. Wang, Y. Li, S. Jiang, N. Yu, G. Zhou, Prognosis and chemotherapy drug sensitivity in liver hepatocellular carcinoma through a disulfidptosis-related lncRNA signature, Sci. Rep. 14 (1) (2024) 7157.
[31] Z. Song, X. Cao, X. Wang, Y. Li, W. Zhang, Y. Wang, et al., A disulfidptosis-related lncRNA signature for predicting prognosis and evaluating the tumor immune microenvironment of lung adenocarcinoma, Sci. Rep. 14 (1) (2024) 4621.
[32] W. Xue, K. Qiu, B. Dong, D. Guo, J. Fu, C. Zhu, et al., Disulfidptosis-associated long non-coding RNA signature predicts the prognosis, tumor microenvironment, and immunotherapy and chemotherapy options in colon adenocarcinoma, Cancer Cell Int. 23 (1) (2023) 218.
[33] L. Zhang, Z. Zhang, X. Zheng, Y. Lu, L. Dai, W. Li, et al., A novel microRNA panel exhibited significant potential in evaluating the progression of laryngeal squamous cell carcinoma, Noncoding RNA Res 8 (4) (2023) 550–561.
[34] Y. Zheng, J. Wu, B. Yan, Y. Yang, H. Zhong, W. Yi, et al., Identification of a two metastasis-related prognostic signature in the process of predicting the survival of laryngeal squamous cell carcinoma, Sci. Rep. 13 (1) (2023) 13513.
[35] X. Zheng, W. Gao, Z. Zhang, X. Xue, M. Mijiti, Q. Guo, et al., Identification of a seven-lncRNAs panel that serves as a prognosis predictor and contributes to the malignant progression of laryngeal squamous cell carcinoma, Front. Oncol. 13 (2023) 1106249.
[36] C. Murdoch, M. Muthana, S.B. Coffelt, C.E. Lewis, The role of myeloid cells in the promotion of tumour angiogenesis, Nat. Rev. Cancer 8 (8) (2008) 618–631.
[37] G. Varricchi, M.R. Galdiero, S. Loffredo, V. Lucarini, G. Marone, F. Mattei, et al., Eosinophils: the unsung heroes in cancer? OncoImmunology 7 (2) (2018) e1393134.
[38] Q. Sun, X. Qin, J. Zhao, T. Gao, Y. Xu, G. Chen, et al., Cuproptosis-related LncRNA signatures as a prognostic model for head and neck squamous cell carcinoma, Apoptosis 28 (1–2) (2022) 247–262.
[39] L. Tang, Z. Huang, H. Mei, Y. Hu, Immunotherapy in hematologic malignancies: achievements, challenges and future prospects, Signal Transduct. Targeted Ther. 8 (1) (2023) 306.
[40] S.L. Topalian, P.M. Forde, L.A. Emens, M. Yarchoan, K.N. Smith, D.M. Pardoll, Neoadjuvant immune checkpoint blockade: a window of opportunity to advance cancer immunotherapy, Cancer Cell 41 (9) (2023) 1551–1566.
[41] G. Mountzios, J. Remon, L.E.L. Hendriks, R. Garcia-Campelo, C. Rolfo, P. Van Schil, et al., Immune-checkpoint inhibition for resectable non-small-cell lung cancer - opportunities and challenges, Nat. Rev. Clin. Oncol. 20 (10) (2023) 664–677.
[42] B. Burtness, K.J. Harrington, R. Greil, D. Soulieres, M. Tahara, G. de Castro Jr., et al., Pembrolizumab alone or with chemotherapy versus cetuximab with chemotherapy for recurrent or metastatic squamous cell carcinoma of the head and neck (KEYNOTE-048): a randomised, open-label, phase 3 study, Lancet 394 (10212) (2019) 1915–1928.
[43] J.W. Carlisle, C.E. Steuer, T.K. Owonikoko, Saba NF an update on the immune landscape in lung and head and neck cancers, Ca - Cancer J. Clin. 70 (6) (2020) 505–517.
[44] S. McBride, E. Sherman, C.J. Tsai, S. Baxi, J. Aghalar, J. Eng, et al., Randomized phase II trial of nivolumab with stereotactic body radiotherapy versus nivolumab alone in metastatic head and neck squamous cell carcinoma, J. Clin. Oncol. 39 (1) (2021) 30–37.